Discover Concrete and Cement

RESEARCH Open Access

Pozzolanic reactivity and mortar performance of sugarcane bagasse and sawdust ashes in lime based binders

Odiwuor Vincent Onyango[1*], Enos W. Wambu[1], Maurice O. Okoth[1] and Pius K. Kipkemboi[1]

*Correspondence:
Odiwuor Vincent Onyango
vincentodiwuor623@gmail.com
[1]Department of Chemistry and Biochemistry, University of Eldoret, P. O. Box 1125-301, Eldoret, Kenya

Abstract

The growing energy demand, rising production costs, and environmental impacts associated with ordinary Portland cement have intensified the search for sustainable, low-carbon binders. Lime–pozzolana systems incorporating agricultural waste ashes present a viable alternative; however, their development is often based primarily on strength results, limiting insight into the role of material structure and reactivity. This study comparatively evaluates sugarcane bagasse ash (SCBA) and sawdust ash (SDA) as supplementary cementitious materials in lime-based binders, with emphasis on linking physicochemical properties to performance. The ashes were produced under controlled calcination at 600–700 °C and characterized for oxide composition, mineralogy, particle size distribution, specific surface area, and loss on ignition. SCBA exhibited a high combined content of SiO_2 + Al_2O_3 + Fe_2O_3 (86.60%) and was predominantly amorphous, whereas SDA showed a significantly lower content (23.16%), higher loss on ignition (15.33%), and a largely crystalline structure, despite possessing a higher specific surface area. Pozzolanic activity was assessed via electrical conductivity measurements. The results revealed faster early reactivity for SDA, attributed to its higher surface area, while SCBA demonstrated more sustained reactivity due to its high amorphous silica content. At 28 days, SCBA–lime mortars achieved compressive strengths of 2.98–3.72 MPa, compared to 1.51–2.52 MPa for SDA–lime mortars across pozzolan-to-lime ratios of 3:1 to 1:1. Similarly, SCBA mortars exhibited higher bulk density (930.6 kg/m^3) and lower water absorption (14.14%) than SDA mortars (812.4 kg/m^3 and 18.14%, respectively). All mixes exceeded the minimum strength requirement of 2 MPa for lime–pozzolana binders, although they remained significantly lower than the OPC control (48.06 MPa). Overall, SDA enhances early-age reactivity, whereas SCBA provides superior long-term mechanical performance. These findings establish a clear relationship between material characteristics, pozzolanic behavior, and mortar performance, offering practical guidance for the selection of locally available agricultural ashes in sustainable construction.

Keywords Lime binder, Pozzolanic activity, Sugarcane bagasse ash, Sawdust ash, Supplementary cementitious materials

1 Introduction

Global demand for cement continues to rise, driven by rapid urbanization, population growth, and expanding infrastructure, especially in developing economies. Recent industry assessments confirm steady increases in both production and consumption worldwide [1]. Ordinary Portland Cement (OPC) remains the primary construction binder, yet its production requires substantial energy and carries a heavy environmental cost. The manufacture of clinker involves calcining limestone and clay at temperatures above 1300 °C, a process that consumes significant amounts of fossil fuel and releases considerable carbon dioxide [2]. The cement industry is responsible for about 5–8% of global human-generated carbon dioxide emissions while also contributing to resource depletion and air pollution. The global construction sector is under growing pressure due to the substantial energy consumption, environmental consequences, and carbon emissions linked to the production of OPC. These environmental pressures pose a major sustainability challenge for the construction sector [3, 4].

In response, research has increasingly focused on reducing dependence on ordinary Portland cement without compromising material performance. The increasing impact of environmental degradation and greenhouse gas emissions highlights the urgent need for sustainable construction materials, with recycling serving as a key strategy in advancing circular economy objectives [5]. One widely explored strategy involves the partial or complete replacement of clinker with supplementary cementitious materials (SCMs). Materials including fly ash, ground granulated blast furnace slag, silica fume, and rice husk ash have been widely investigated for their ability to reduce energy consumption and carbon emissions while also decreasing clinker content and enhancing durability [6–9].

However, declining coal-based power generation, changes in industrial activity, and growing transportation distances are affecting the long-term supply, cost, and environmental benefits of these conventional by-products. Scrivener et al. [3]. argue that materials such as ground granulated blast furnace slag, fly ash, waste glass, and silica fume are unlikely to satisfy the growing demand for supplementary cementitious materials in cement production. They further contend that ashes generated from agricultural activities alone would also be insufficient to meet this demand. Consequently, attention has shifted toward locally available and potentially sustainable agricultural and industrial waste ashes as alternative pozzolanic resources [8].

Among these agro-industrial waste ashes, sugarcane bagasse ash (SCBA) and sawdust ash (SDA) have received growing attention. Sawdust ash, produced from timber residues, shows variable pozzolanic performance depending on the type of biomass, burning conditions, and remaining carbon content [8]. Sugarcane bagasse ash, generated during sugar processing, can yield highly reactive amorphous silica when properly calcined. Numerous studies worldwide have examined sugarcane agro-waste because of its significant pozzolanic oxide content. However, the characteristics of SCBA and its optimum replacement levels differ considerably across regions. For instance, the combined pozzolanic oxides of SiO_2 + Al_2O_3 + Fe_2O_3 have been reported to range widely, from as low as 27.2% to as high as 88% [10–11]. Hossain et al. [12]. investigated the incorporation of industrial by-products such as SCBA in the production of sustainable construction binders. Their study reported improvements in hydration behavior, mechanical strength, and microstructural densification. The findings indicated increased pozzolanic reactivity

and progressive strength gain, highlighting the capacity of these waste-derived materials to contribute to sustainable development and climate mitigation objectives.

Costa *et al.* [13]. reported that partially replacing Portland cement clinker with SCBA improves the mechanical properties of the composite and contributes to a more sustainable construction material. Many other investigations have assessed SCBA and SDA separately as supplementary cementing materials, mainly within ordinary Portland cement systems. These studies have reported improvements in strength and durability when composition and processing are carefully controlled [9, 14–18]. Nevertheless, studies directly comparing these two ashes in lime-based binders under the same experimental conditions are still limited.

Furthermore, most previous research has relied heavily on compressive strength measured at later ages. Although compressive strength is an important indicator, it does not fully explain early reaction mechanisms or clarify whether performance depends more on surface area, chemical makeup, or the amount of amorphous material. Consequently, the links between structure, reactivity, and performance in lime–pozzolana systems are not yet fully established. Measuring electrical conductivity in saturated calcium hydroxide solutions provides a rapid way to monitor early pozzolanic activity by tracking the consumption of calcium and hydroxide ions in real time. Unlike conventional strength testing, this method helps distinguish between rapid surface-controlled reactions and slower, chemically governed processes. Despite its potential, few comparative studies have combined conductivity-based testing with detailed chemical, mineralogical, and mechanical analyses of agricultural ashes in lime-based systems.

This study addresses these gaps through a controlled comparative evaluation of SCBA–lime and SDA–lime binders produced under identical calcination and curing conditions. The primary objective is to correlate early-age pozzolanic reactivity, quantified via electrical conductivity, with ash composition, mineralogy, specific surface area, and 28-day mortar performance. It is hypothesized that materials with higher specific surface area will exhibit faster early-age pozzolanic reactions due to increased reactive surface exposure, and long-term compressive strength will be governed primarily by reactive oxide content and amorphous phase availability (as in SCBA), rather than surface area alone. By systematically testing these hypotheses and benchmarking against OPC mortars, this study advances current SCBA and SDA research beyond strength-based evaluation, establishes clearer structure–reactivity–performance relationships, and provides performance-informed guidance for selecting locally available agricultural ashes as sustainable lime-based construction materials.

2 Materials and methods

2.1 Materials

Sugarcane bagasse (SCB) for this study was obtained from Butali Sugar Company Limited (Kakamega, Kenya). Sawdust was randomly collected from two commercial sawmills on the outskirts of Eldoret City, Kenya. To prevent sand contamination, samples were carefully collected by putting fresh sawdust ash into the bags. Commercial Ordinary Portland Cement 42.5 conforming to KS EAS 18 – 1: 2017 [19] was supplied by Simba Cement Company Limited (Nakuru, Kenya) for control purposes. Standard river sand was used as fine aggregate for mortar preparation. Deionized water was used throughout

the study. Hydrated commercial lime ($Ca(OH)_2$) conforming to KS EAS 18 – 1:2017 [19] was supplied by Laboklin Chimique Company Limited.

2.2 Methods

2.2.1 Sample preparation

Sugarcane bagasse samples were ground using an HFM 100 grinder (Beijing Grinder Instrument Co., Ltd., Beijing, China) under dry grinding conditions. The material was milled for 15 min at a rotational speed of 300 rpm to achieve a particle size passing a 90 μm sieve. Sugarcane bagasse samples were rinsed with distilled water to remove sand and impurities, then oven-dried at 110 °C for 24 h. Collected sawdust (SD) from local sawmills in Eldoret was sun-dried for ten days to reduce moisture content naturally, minimizing energy use while preventing thermal decomposition of volatile organics. Sand samples were washed with deionized water and sun-dried for two days. Oven-drying was not required because sand's low organic content and coarse particle size allow adequate moisture removal under ambient conditions without affecting grading or water absorption.

2.2.2 Calcination of the pozzolans

The dried SCB was converted into ash through controlled calcination in an air atmosphere in a muffle furnace (Advantec KL-420, Tokyo, Japan) under three separate conditions: 600 °C for 2 h, 600 °C for 1 h, and 700 °C for 1 h. A controlled heating rate of approximately 10 °C/min was applied. These conditions were selected to evaluate the influence of calcination temperature on pozzolanic reactivity while ensuring complete removal of organic matter and avoiding excessive crystallization. The resulting SCBA was cooled naturally inside the furnace to room temperature for 24 h and then ground under dry conditions using an HFM 100 grinder (Beijing Grinder Instrument Co., Ltd., Beijing, China) for 15 min to achieve a particle size passing a 75 μm sieve and stored in airtight containers.

The collected sawdust was sun-dried for ten days to reduce moisture content. The dried SD was calcined in a laboratory muffle furnace under controlled conditions. Calcination was performed under an oxidizing atmosphere using three different temperature–time regimes: 600 °C for 1 h, 600 °C for 2 h, and 700 °C for 1 h. A heating rate of approximately 10 °C/min was applied to reach the target temperature. After completion of the calcination period, the ash was allowed to cool naturally inside the furnace to room temperature. The resulting SDA was then ground under dry conditions for 15 min to pass a 75 μm sieve and stored in airtight containers. These controlled regimes were selected to evaluate the influence of temperature and residence time on ash reactivity and phase composition.

2.2.3 Physical, chemical, and mineralogical analysis

Particle size distribution (PSD) was assessed using a conventional mechanical sieve analyzer in accordance with KS 02 1263 [20]. The analysis was primarily conducted to determine the percentage of material passing the 90 μm sieve and to verify compliance with fineness requirements. It is acknowledged that sieve analysis provides limited resolution for ultrafine particles (< 75 μm), and therefore the reported PSD reflects coarse fraction grading rather than full submicron distribution. Although sieve analysis was used for

grading control, Brunauer–Emmett–Teller (BET) specific surface area (SSA) analysis was employed to better capture fineness characteristics of the ashes. This was accomplished using a BET nitrogen adsorption analyzer (Gemini 2375 V). The BET surface area was determined using the multipoint method over a relative pressure (P/P_o) range of 0.05–0.30. Elemental composition for both the pozzolans and control OPC was determined with an XRF spectrometer (Epsilon 3XLE, Malvern Panalytical, Almelo, Netherlands). The mineralogical and amorphous characteristics of the pozzolans were examined using X-ray diffraction (Bruker AXS GmbH, Karlsruhe, Germany). XRD characterization was conducted on SCBA and SDA samples calcined at 600 °C for 1 h, as these ashes exhibited the most favorable pozzolanic reactivity.

2.2.4 Loss on ignition (LOI)

One gram of obtained raw pozzolans was oven-dried at 110 °C for 1 h, then heated in an air atmosphere in a muffle furnace at 1000 °C for 1 h, cooled in a desiccator, and reweighed. Percentage loss on ignition (LOI) was calculated according to the procedure described elsewhere in the literature [21].

2.2.5 Evaluation of pozzolanic activity

Evaluation of the pozzolanic activity test was carried out using a modified procedure of Marangu [22]. A saturated calcium hydroxide solution was prepared by adding 0.8 g of $Ca(OH)_2$ to 200 mL of distilled water in a 250 mL beaker, maintained at 38 ± 1 °C on a hot magnetic plate with continuous stirring. The solution's electrical conductivity was measured using a conductivity meter. After the lime-water system stabilized, 5 g of ground pozzolana were added and stirred for two minutes. Conductivity measurements were taken every 30 min for 4 h. A pozzolana–water system without lime was also tested, and its contribution was subtracted from the lime–pozzolana readings to obtain corrected conductivity values. The procedure was repeated for different temperatures and calcination times.

To quantitatively classify pozzolanic reactivity, percentage conductivity loss was calculated at defined intervals (30, 120, and 240 min) relative to the initial conductivity of the saturated calcium hydroxide solution. Following benchmarks established in previous conductivity-based studies on known pozzolans like rice husk ash, sugarcane bagasse ash, and metakaolin, the following classifications were adopted: High reactivity: ≥ 30% conductivity loss at 30 min, Moderate reactivity: 15–30% conductivity loss at 30 min and low reactivity: < 15% conductivity loss at 30 min [11, 21–24].

2.2.6 Molding and curing the test mortar prisms

Mortar prisms were prepared in compliance with the Kenyan standard, KS EAS 2168-1 [25]. Three mortar prisms measuring 160 mm by 40 mm by 40 mm for each test sample were made simultaneously. This was accomplished by using a trowel to mix 1350 g of graded sand and 450 g of pozzolana lime mixture (3:1) on a non-porous plate for one minute. Only SCBA and SDA calcined at 600 °C for 2 h were used for mortar preparation because preliminary tests on early-age pozzolanic activity indicated these samples provided the best balance of reactivity (Table 1). Water was added gradually to the pozzolana–lime–sand mixture in a stainless-steel bowl to achieve a workable mortar consistency.

Table 1 Percentage conductivity loss (%) of SCBA and SDA under different calcination conditions

Time (min)	SCBA (600 °C–1 h)	SCBA (600 °C–2 h)	SCBA (700 °C–1 h)	SDA (600 °C–1 h)	SDA (600 °C–2 h)	SDA (700 °C–1 h)
30	21	24	14	63	65	69
120	26	31	23	65	72	78
240	30	34	28	64	71	75

Workability was assessed using the flow table method following KS EAS 148-1 [26], with a target flow diameter of 110–120 mm, ensuring adequate spreadability for molding without segregation. Although detailed rheological characterization (e.g., yield stress and plastic viscosity) was beyond the scope of this study, the fresh-state behavior of the mortars was indirectly evaluated using flow table measurements. Workability was controlled by adjusting the water-to-binder (w/b) ratio to achieve a consistent target flow of 110 ± 5 mm for all mixes. This single-point control ensures that variations in mechanical performance are primarily governed by the intrinsic properties of the binders, such as pozzolanic reactivity and ash morphology, rather than differences in workability.

To create a cement mortar with a uniform consistency, mixing was then carried out for an additional 4 min using a trowel. The prepared mortar mixture was carefully placed into grease-lubricated molds and compacted using a laboratory vibrating table for 2 min to remove entrapped air. A curing environment with a relative humidity of greater than 90% was used to store the prisms. In the curing room, the prisms were covered with a flat, impermeable layer of polyethylene paper. After a 24-h period, the prisms were demolded, labeled for identification, and allowed to cure in the air for 28 days at 23 ± 2 °C and 65 ± 5% relative humidity. Air curing was employed because lime cement does not solidify in water, and it takes a long time to cure; therefore, the 3- and 7-day strengths could not be estimated [11]. The process above was repeated with 450 g of pozzolana-lime mixes in ratios of 2:1 and 1:1.

The pozzolana-to-lime ratios of 3:1, 2:1, and 1:1 were selected based on both chemical and practical considerations. Chemically, varying the ratio enables evaluation of different levels of calcium hydroxide availability for the pozzolanic reaction, with higher pozzolana content (3:1) representing a more demanding condition for reactive silica consumption. Practically, these ratios are consistent with traditional lime mortar practices, where binder proportions are adjusted according to the reactivity of supplementary materials. Similar ranges have also been widely used in studies on agricultural ashes, providing a reliable basis for comparison [11, 21]. For reference purposes, OPC mortar prisms were also made; however, this time the OPC was mixed with sand alone, and they were cured in water for 28 days.

The curing regimes were selected to suit the optimal development conditions of each binder system. OPC mortars were water-cured to promote continuous hydration of the silicate phases, whereas lime-based mortars were air-cured at 23 ± 2 °C and 65 ± 5% relative humidity. Air curing is necessary for lime–pozzolana systems to enable carbonation through atmospheric CO_2 uptake and to minimize the leaching of calcium hydroxide prior to completion of the pozzolanic reaction. Therefore, comparisons between the two systems reflect their performance under respective optimal curing conditions and are not strictly equivalent due to the differing curing mechanisms. A total of 36 pozzolana-lime mortars and 9 OPC mortars were prepared.

2.2.7 Bulk density

The bulk densities of the mortar prisms were determined according to the requirements of BS 1881 [27]. After 28 days of curing, the samples were dried at 60 ± 2 °C until their mass remained constant. The mass (m_o, kg) of the specimen was determined after it had cooled down to room temperature (25 °C). The dimensions of the mortar prisms were measured, and bulk volume was calculated using the geometry approach (multiplying the length, breadth, and height of the specimens). The final dry density of the mortar was calculated as a mass-to-volume ratio.

2.2.8 Water absorption

The testing procedure for water absorption capacity followed the guidelines of BS 1881 – 122 [28]. Before immersion, the 28-day cured mortar samples were placed in a ventilated oven at a temperature of 60 ± 5 °C and dried until they reached a constant weight. After drying, they were allowed to cool in a desiccator, and the dry mass of each sample was recorded as m_1. The samples were then immersed in a sealed container filled with water for 48 h. During immersion, the specimens were inclined at an angle of about 45° to help release any trapped air bubbles. Once submerged, they were positioned vertically, marking the start of the test. After the 48-hour immersion period, the samples were removed, gently wiped with a damp cloth, and their saturated mass was measured and recorded as m_2. The result of this test is the percentage of water absorbed by the samples, which is determined using Eq. 1.

$$W = \frac{m2 - m1}{m1} \times 100 \tag{1}$$

Bulk density and water absorption measurements were performed on mortar specimens prepared using SCBA and SDA calcined at 600 °C for 2 h.

2.2.9 Compressive strength determination

The analysis of compressive strength of all the mortar prisms was conducted in compliance with the requirements of KS EAS 148-1 [26]. The compressive strength of the cured specimens was determined using a universal testing machine for compression (SSC-546, Instron, Norwood, USA) in accordance with standard testing procedures. The mortar prism was oriented lengthwise in the compressive machine so that its end face overhangs the platens or auxiliary plates by around 10 mm and is centered on the platens of the compressive equipment within ± 0.5 mm. Over the course of the load application, the load was gradually increased at a rate of 2400 ± 200 N/s till fracture. For each test regimen, results were obtained in triplicate. The value of compressive strength was determined and reported in MPa.

2.3 Data analyses

All tests were conducted in triplicate, and the mean and standard deviation values were obtained from triplicate measurements in Microsoft Excel. The compressive strength results of the SCBA–lime and SDA–lime mortars were compared statistically using independent two-sample t-tests at a 95% confidence level ($\alpha = 0.05$). The remaining data are reported as mean values with their corresponding standard deviations, without applying further inferential statistical analyses.

Table 2 Physical properties of RHA, SCBA, and OPC

Sample	Specific gravity	Specific Surface Area (m^2/g)	Mean particle size (μm)
OPC	2.9	0.90	365
SCBA	2.0	33.29	252
SDA	1.8	83.14	207

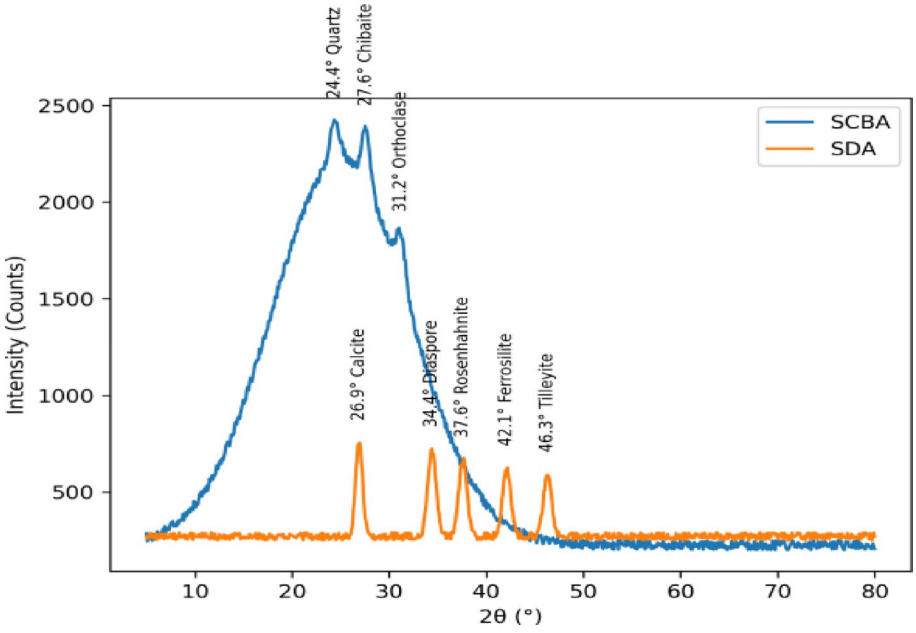

Fig. 1 Combined XRD patterns of SCBA and SDA

The results were presented pictorially in statistical distribution tables and line and bar graphs as appropriate.

3 Results and discussion

3.1 Physical characterization of the materials

The results for specific gravity, mean particle size distribution (PSD), and BET specific surface area values for SCBA, SDA, and OPC are presented in Table 2. Table 2 shows that OPC exhibits the lowest BET specific surface area compared to SDA and SCBA, reflecting its dense particle structure and compact clinker phases. Previous investigations have shown that agro-industrial ashes typically possess a relatively high specific surface area. This characteristic is largely associated with their porous morphology and significant amorphous phase content, which together contribute to improved pozzolanic reactivity [29, 30]. Consistent with these reported trends, the SCBA and SDA examined in the present study also displayed comparatively high SSA values, aligning well with observations documented in the literature.

Among the ashes, SDA possesses a higher SSA than SCBA. Higher SSA facilitates early pozzolanic reactions by enhancing dissolution rates and improving contact with calcium hydroxide, promoting faster formation of secondary cementitious phases. Accordingly, the lower SSA of SCBA may limit its early-age reaction relative to SDA [30]. However, pozzolanic performance also depends on chemical composition and silica reactivity [31]. Despite its lower SSA, SCBA demonstrates strong long-term pozzolanic potential due to its high amorphous silica content. XRD analysis (Fig. 1) confirmed that SCBA contains

a substantial proportion of amorphous silica inferred from the broad hump between approximately 15° and 35° 2θ, supporting sustained pozzolanic activity and improved long-term strength development.

The specific surface area of the SCBA sample investigated in this study (33.29 m^2/g) is in close agreement with values reported in previous studies. For instance, Yaseen [32] documented an SSA of 30.55 m^2/g, while Pavía and Figueiredo [30] reported a value of 25.64 m^2/g for SCBA. In contrast, the SSA obtained in the present work is considerably higher than the 2.9 m^2/g reported by Nayak et al. [33]. Such discrepancies in SSA values may be attributed to differences in particle morphology, as SCBA particles can occur in diverse shapes, including angular, prismatic, spherical, and fibrous forms [32]. Variations in SSA reported by Jittin and Bahurudeen [34] further underscore the influence of calcination, grinding, and processing on ash fineness and reactivity. SSA increases with decreases in mean particle size.

3.2 Chemical analysis results

Table 3 summarizes the average oxide composition and loss on ignition of SDA, SCBA, and OPC, expressed as mass percentages. The pozzolanic potential of a material is largely determined by the combined content of SiO_2, Al_2O_3, and Fe_2O_3, which react with calcium hydroxide to form cementitious hydration products. SCBA exhibited a high combined oxide content of 86.60%, meeting the requirements of KS EAS 18 – 1 [19] and ASTM C618 [35]. The XRF results in Table 3 indicate a clear chemical distinction between the two agro-waste ashes. The high silica content of SCBA enhances its capacity for sustained pozzolanic reactions with the lime binder. The pozzolanic oxide content of SCBA determined in this study falls within the range commonly reported for properly processed SCBA in the literature. Previous studies indicate that, under comparable calcination conditions, these values generally vary between 78% and 89% [11, 30, 32].

In contrast, SDA showed a much lower combined oxide content of 23.16%, below the thresholds specified for conventional pozzolans. Literature reports for SDA's combined oxide contents are highly variable, ranging from 13.03% to 88.32% [36–42], reflecting differences in biomass source, species, growth conditions, and combustion methods. The SDA used in this study lies toward the lower end of this spectrum. High MgO content can cause volumetric instability and microcracking [43]. However, in this study, MgO levels in SCBA, SDA, and OPC were all below 5%, reducing this risk. Total alkalis ($Na_2O + K_2O$) were below 1.5% for all materials, consistent with acceptable limits and minimizing the potential for alkali-related cracking [44]. OPC's alkali content of 0.6% is within typical commercial ranges.

SCBA's LOI complied with ASTM C618 [35], indicating minimal residual carbon and satisfactory workability. Similar LOI values have been reported for properly calcined SCBA. SDA, however, had a high LOI of 15.33%, likely due to unburnt carbon and residual organics, consistent with other studies of incompletely combusted biomass [45]. Elevated LOI can negatively affect workability and pozzolanic reactivity. The elevated LOI and lower combined oxide content in SDA indicate that its role in the mortar matrix is partly physical, acting as a filler and nucleation site, and partly chemical, whereas SCBA functions as a more effective supplementary cementitious material. OPC's LOI was below 5%, in line with KS EAS 18 – 1 [19] and typical commercial cement values.

Table 3 Chemical composition of SDA, SCBA, and control OPC

Material	SiO_2	Al_2O_3	Fe_2O_3	CaO	MgO	K_2O	Na_2O	LOI	$SiO_2+Al_2O_3+Fe_2O_3$
SDA	13.22 ± 0.01	6.25±	3.68 ± 0.05	41.4 ± 0.05	1.16 ± 0.05	1.27 ± 0.05	0.32 ± 0.01	15.33 ± 0.02	23.16 ± 0.02
SCBA	84.61 ± 0.04	0.42 ± 0.01	0.74 ± 0.02	2.59 ± 0.03	–	0.94 ± 0.02	0.90 ± 0.01	11.58 ± 0.02	85.77 ± 0.04
OPC	29.69 ± 0.02	5.10 ± 0.01	3.54 ± 0.05	62.51 ± 0.02	2.21 ± 0.05	0.62 ± 0.05	0.16 ± 0.05	26.3 ± 0.02	–

The XRF results (Table 3) provide a fundamental basis for interpreting the observed mortar performance. The high content of reactive oxides in SCBA classifies it as a high-quality pozzolan in accordance with ASTM C618 [35], promoting the formation of dense calcium silicate hydrate (C–S–H) gels. In contrast, although SDA contains a lower proportion of pozzolanic oxides, its XRF profile indicates a heterogeneous mineral composition that, together with its high specific surface area, contributes to the rapid initial conductivity loss observed during the early stage of the reactivity tests. These findings suggest that SDA primarily enhances early-age reactivity, while SCBA supplies the chemical composition necessary for long-term strength development and structural integrity.

3.3 Mineralogical analysis results

Although sugarcane bagasse and sawdust are plant-derived, calcination removes their organic matter, yielding predominantly inorganic ashes. The mineralogical composition of these ashes strongly affects their pozzolanic reactivity in lime-based binders; therefore, X-ray diffraction analysis was performed to identify the crystalline and amorphous phases in SCBA and SDA. The XRD pattern of SCBA indicates a mixture of crystalline and amorphous phases. Minor diffraction peaks correspond to quartz, orthoclase, and chibaite. The broad hump between 20° and 35° 2θ indicates the presence of amorphous silica typical of reactive pozzolanic materials. This amorphous component is recognized as the most reactive form of silica in pozzolanic systems [45]. Similar XRD features have been reported for SCBA calcined under controlled conditions [46–47], confirming that the mineralogical composition observed in this study aligns with reactive SCBA reported in the literature.

By contrast, the SDA pattern exhibits a predominantly crystalline structure, with sharp peaks attributed to calcite ($CaCO_3$) and additional phases including diaspore, rosenhahnite, ferrosilite, and tilleyite. In contrast to SCBA, the XRD pattern of SDA displays a much less distinct amorphous hump within the 20°–35° 2θ range, suggesting that the material contains a smaller proportion of amorphous silica. The limited amorphous phase indicates weaker pozzolanic activity, which could explain the relatively lower strength development recorded in SDA–lime mortars. Sustained pozzolanic reactions are largely governed by the presence of reactive oxides (SiO_2 + Al_2O_3 + Fe_2O_3) in an amorphous state. The relatively lower amorphous fraction in SDA, together with its reduced pozzolanic oxide content, may explain its comparatively weaker long-term performance. Nevertheless, the presence of silicate and aluminate phases suggests that SDA can still participate in limited pozzolanic reactions, particularly at early ages or when finely ground, as noted in previous studies [48].

3.4 Pozzolanic activity test results

Pozzolanic activity was assessed by measuring the reduction in electrical conductivity of saturated calcium hydroxide solutions after introducing SCBA and SDA calcined under controlled conditions. The variation in conductivity with time is shown in Figs. 2, 3 and 4. Among the thermal regimes considered, calcination at 600 °C for 2 h resulted in the greatest conductivity loss, signifying enhanced early-age reactivity. The extended heating period likely facilitated more complete removal of organic constituents. This favored the development of reactive amorphous silica while maintaining structural disorder.

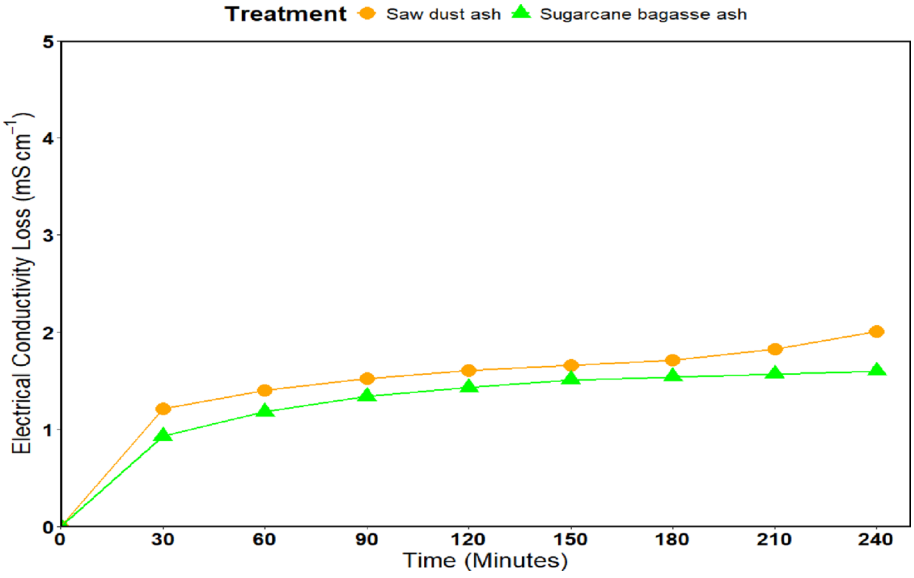

Fig. 2 Pozzolanic activity of SDA & SCBA samples calcined for 1 h at 600 °C

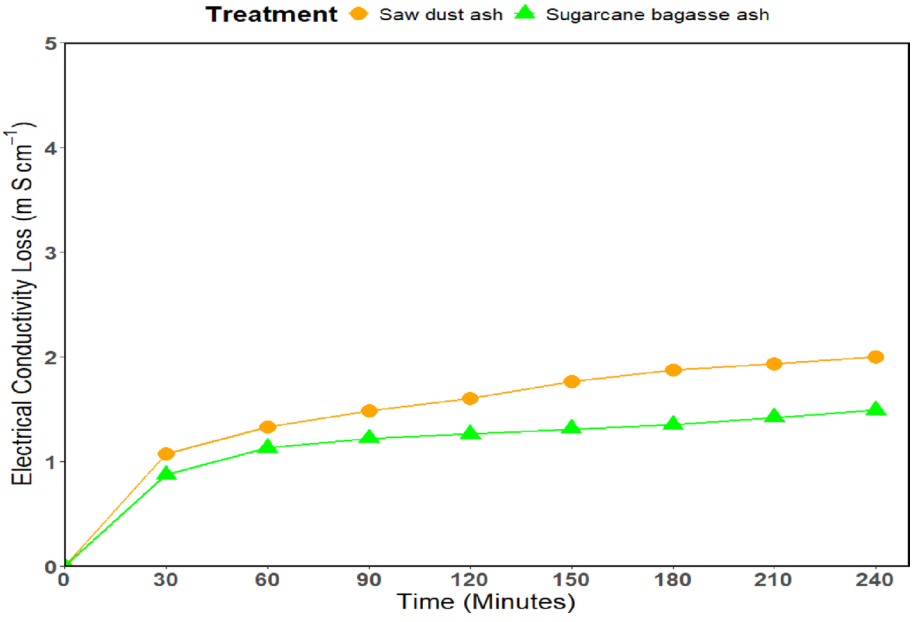

Fig. 3 Pozzolanic activity of SDA & SCBA samples calcined for 2 h at 600 °C

By comparison, shorter calcination periods may not sufficiently activate the material, whereas higher temperatures (700 °C) can induce partial crystallization or particle sintering, thereby leading to a decrease in the available reactive surface and limiting ionic interaction within the lime solution [24].

Both SCBA and SDA produced a measurable reduction in electrical conductivity. This decrease indicates the consumption of Ca^{2+} and OH^- ions during the pozzolanic reaction, as reactive SiO_2 and Al_2O_3 interact with $Ca(OH)_2$ to form secondary calcium silicate hydrate (C–S–H) [23, 49]. During the first 30 min (Phase 1), all samples showed a marked drop in conductivity. SDA demonstrated a greater initial reduction than SCBA, which may be associated with its higher specific surface area. SDA calcined at 600 °C for

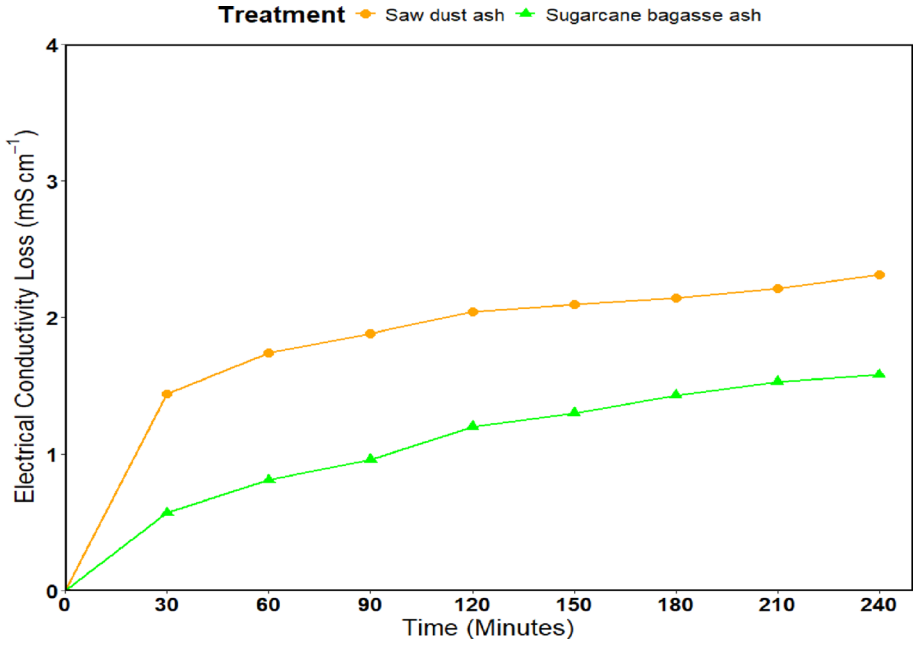

Fig. 4 Pozzolanic activity of SDA & SCBA samples calcined for 1 h at 700 °C

2 h achieved a 65% conductivity loss at 30 min. This corresponds to high early reactivity under the adopted criteria. SCBA recorded 24% at the same interval, indicating moderate early reactivity. In Phase 2 (120–240 min), SDA calcined at 600 °C for 2 h attained conductivity losses of 72% at 120 min and 78% at 240 min. In contrast, SCBA exhibited 31% conductivity loss at 120 min and 34% at 240 min. Comparable trends have been reported elsewhere by Assumptor et al. [11]. They observed that RHA showed the highest conductivity reduction (77%), followed by clay (56%), while SCBA exhibited 26%. Similarly, John [21] reported a 1.3 mS/cm decrease in electrical conductivity for rice husk ash.

Notably, despite SDA having a lower combined pozzolanic oxide content (23.16%) and a predominantly crystalline structure, it displayed a greater early-stage conductivity loss than SCBA. This pronounced reduction is likely related to its higher specific surface area and faster dissolution rate, which enhance early Ca^{2+} consumption. Thus, conductivity loss primarily reflects reaction kinetics rather than total reactive oxide content [24, 31]. These findings underscore the importance of particle size and surface area in governing early pozzolanic response, consistent with Walker and Pavía [31]. The reactivity observed for SDA aligns with earlier studies [50–51]. However, reduced performance has been noted in materials with high LOI or low silica content [52–53]. Although SCBA contains a higher proportion of amorphous silica and greater total pozzolanic oxide content, electrical conductivity measurements mainly capture early reaction rates rather than ultimate pozzolanic capacity. Accordingly, SCBA, despite its richer amorphous composition, may exhibit slower initial ion consumption. It contributes more significantly to sustained lime–pozzolana reactions and long-term strength development. Therefore, conductivity testing principally evaluates early lime consumption and does not necessarily predict the final pozzolanic potential or mechanical performance of the material.

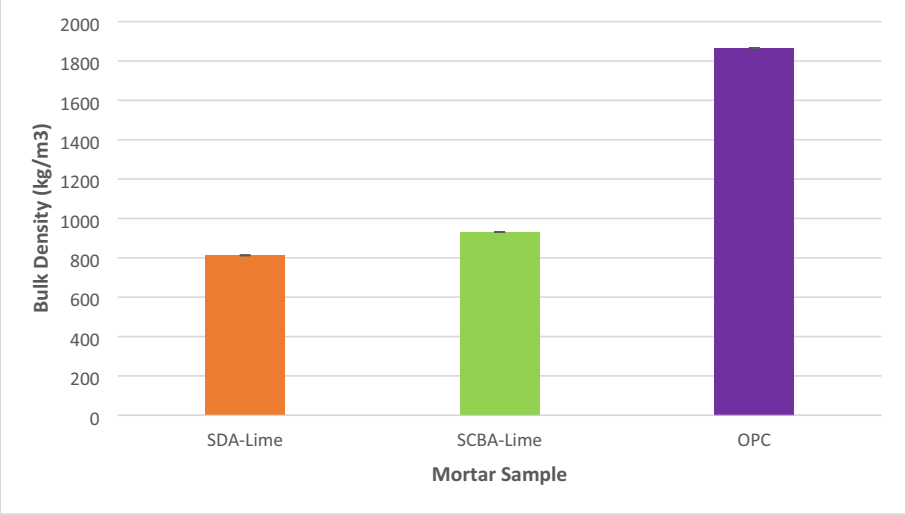

Fig. 5 Bulk densities for various pozzolana-lime mortars and OPC

Table 4 Mechanical analysis test results

Mortar sample	Bulk density (kg/m³)	Water absorption (%)	Compressive strength (MPa)		
			Pozzolan: Lime ratio		
			3:1	2:1	1:1
SDA–Lime	812.4	18.14	1.51 ± 0.02	2.35 ± 0.04	2.52 ± 0.04
SCBA–Lime	930.6	14.14	2.98 ± 0.04	3.56 ± 0.04	3.72 ± 0.06
Control OPC	1865.4	7.21	48.06 ± 0.36		

3.5 Bulk density

Figure 5 and Table 4 present the bulk densities of SCBA–lime, SDA–lime, and OPC mortars after 28 days. OPC exhibited the highest density (1865.4 kg/m³), consistent with typical mortar density ranges of 1500–1900 kg/m³ [54], reflecting its dense clinker phases and high specific gravity. In contrast, SCBA–lime and SDA–lime mortars were substantially lighter, with densities of 930.6 kg/m³ and 812.4 kg/m³, respectively. The lower densities of the pozzolana–lime mortars align with previous reports for lime-based systems [55]. SDA–lime mortar recorded the lowest density, attributed to the low specific gravity, high porosity, and carbon-rich composition of sawdust ash, which increases entrapped air and overall pore volume. Although SDA possesses a comparatively high specific surface area that can enhance early dissolution and promote initial lime consumption, its lower amorphous silica content limits its long-term pozzolanic contribution. Consequently, the formation of secondary C–S–H gel is less pronounced, leading to less matrix densification than in SCBA-based systems.

The SCBA–lime mortar showed a marginally higher density than the SDA–lime mortar.

This difference cannot be attributed solely to particle size. It is also likely influenced by variations in particle morphology, grading characteristics, and specific gravity, which affect packing efficiency and, consequently, the overall bulk density. The reactive silica in SCBA readily interacts with calcium hydroxide released during lime hydration, supporting sustained pozzolanic reactions and long-term strength development. This process promotes the formation of secondary calcium silicate hydrate (C–S–H) gel, which

densifies the matrix by filling capillary voids and refining the pore structure. As a result, porosity decreases and the microstructure becomes more compact.

3.6 Water absorption

Water absorption is an indicator of the volume and interconnectivity of open pores within hardened mortar [55]. As presented in Fig. 6 and Table 4, OPC mortar recorded the lowest absorption value (7.21%), whereas SDA–lime mortar exhibited the highest (18.14%), and SCBA–lime mortar showed an intermediate value (14.14%). Similar patterns have been reported for lime–pozzolana binders in earlier studies [56]. The relatively low absorption observed in OPC mortar is associated with the dense microstructure generated by C–S–H gel during cement hydration, which refines the pore system and restricts capillary water ingress [54]. By contrast, the higher absorption measured in SDA–lime mortar suggests a more open pore network, influenced by the intrinsic porosity of the ash and the possible presence of residual organic matter.

While the larger surface characteristics of SDA may stimulate early-age reactivity, the overall degree of matrix densification remains lower because of the reduced extent of sustained hydrate formation. This results in less effective pore refinement and a comparatively more porous microstructure than that observed in SCBA–lime mortars, thereby leading to higher water absorption. In contrast, SCBA–lime mortar demonstrates moderate absorption, consistent with progressive pore refinement driven by continued pozzolanic reactions in SCBA–lime systems [57]. Although lime–pozzolana mortars generally exhibit higher absorption than OPC mortars, the measured values remain within acceptable limits for applications such as rendering, plastering, and low-rise masonry, in accordance with BS EN 998-1 [58]. Moreover, the relatively higher absorption capacity may offer practical advantages in traditional masonry by enhancing moisture buffering and vapor permeability.

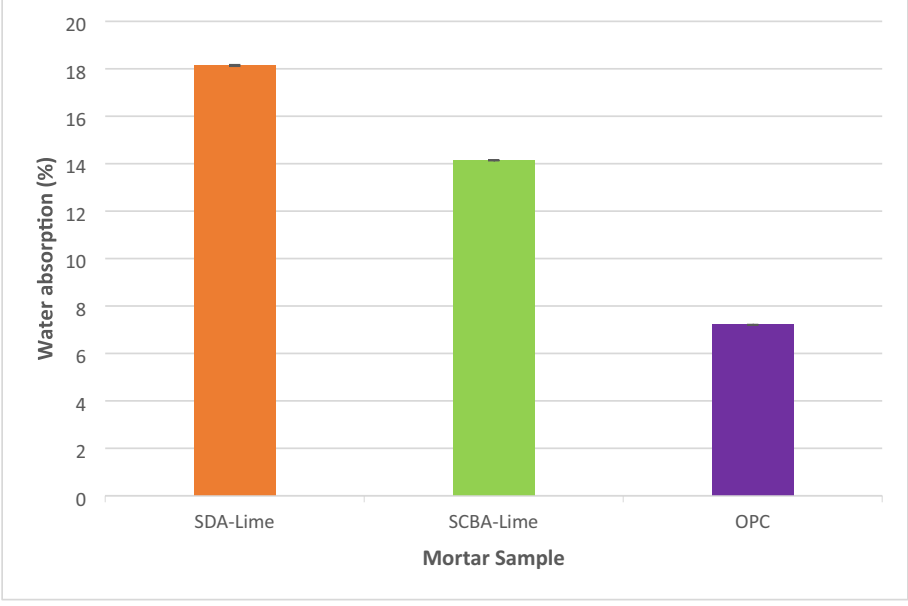

Fig. 6 Water absorption for different pozzolana-lime mortar formulations and OPC

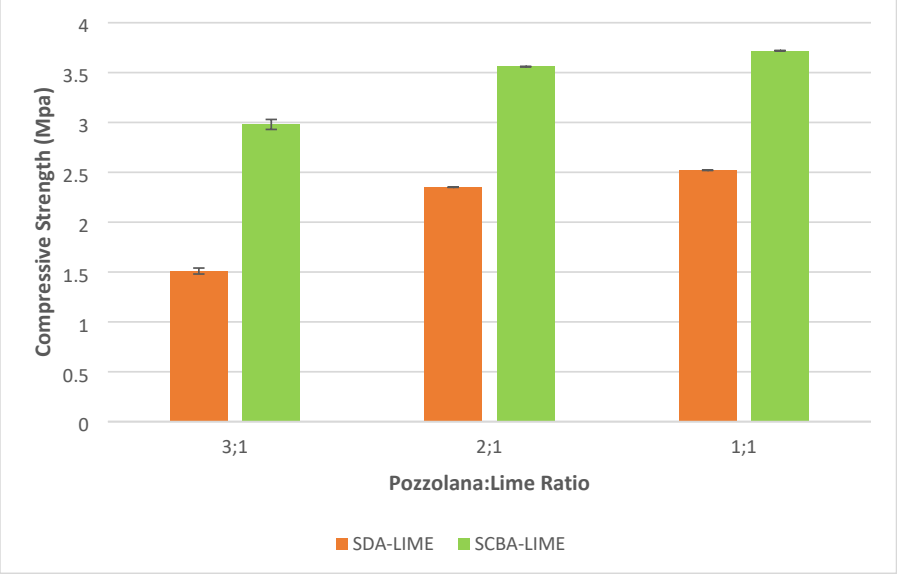

Fig. 7 28-day compressive strength of SCBA-lime and SDA-lime mortars at pozzolana: lime ratios of 3:1, 2:1, and 1:1

3.7 Compressive strength performance

According to Assumptor *et al.* [11]., IS 4098 – 1967 requires a minimum compressive strength of 2 MPa for lime-pozzolana mortars. In the present study, the 28-day compressive strengths of both SCBA–lime and SDA–lime mortars fall within the CS II–CS III range (1.5–7.5 MPa) defined by BS EN 998-1 [58]. This confirms their applicability for rendering, plastering, and low-rise masonry. As shown in Fig. 7; Table 4, strength increased with higher lime proportions in both systems, with the 1:1 pozzolana–lime ratio producing the highest compressive strength values. Comparable behavior has been reported in RHA and calcined clay-based lime binders [21]. Mixes richer in pozzolana (3:1 and 2:1 pozzolana: lime ratios) developed lower strengths. This is due to insufficient lime, which leaves the unreacted particles that contributed to higher porosity [59]. Adequate lime is necessary to maintain pozzolanic reactions.

Independent sample t-tests were conducted to compare compressive strengths of SCBA–lime and SDA–lime mortars at identical pozzolan: lime ratios. Statistically significant differences were observed at all ratios (3:1, 2:1, and 1:1), with SCBA–lime exhibiting higher strength ($p < 0.0001$ in all cases). The 95% confidence intervals did not overlap between corresponding mixes, further confirming the statistical significance of the differences. SCBA–lime mortars consistently outperformed SDA–lime mortars in compressive strength. This agrees with data obtained by Sales and Lima [57], who linked the improved performance of SCBA systems to their higher reactive silica and greater amorphous content. The comparatively lower strength of SDA mortars has been associated with residual organic matter and reduced silica reactivity [14]. Although SDA showed a sharper early reduction in electrical conductivity, indicating faster initial reaction kinetics, SCBA–lime mortars achieved superior 28-day strengths. These results suggest that conductivity predominantly captures early dissolution processes. Long-term strength, however, is governed by the total reactive amorphous fraction and the cumulative development of cementitious hydrates.

The mechanical trends observed can be related directly to the physicochemical properties of the ashes. XRD results revealed a higher proportion of amorphous silica in SCBA than in SDA (Fig. 1), a key factor in sustained pozzolanic performance. The reactive phase consumes calcium hydroxide during hydration, supporting ongoing pozzolanic reactions and secondary C–S–H formation. The accumulation of this hydrate refines the pore structure by filling capillary voids, reducing overall porosity, and producing a denser matrix. As the pore system becomes finer and more compact, load transfer improves and microcrack propagation is restrained. This explains the higher compressive strengths achieved in SCBA-lime mortars. In contrast, the lower amorphous fraction and reduced pozzolanic oxide content of SDA restrict secondary C–S–H formation. This results in limited pore refinement and reduced strength. Chemical composition, mineralogical characteristics, and surface area control lime reaction kinetics, microstructural development, and ultimately the strength of the mortar.

OPC mortar demonstrated substantially higher compressive strength than all lime–pozzolana mortars ($p < 0.0001$), consistent with its rapid hydration of clinker phases (C_3S and C_2S) and early formation of C–S–H gel [60, 61]. Such differences between OPC and lime-based systems are widely documented and stem from fundamental variations in hydration mechanisms and reaction rates.

4 Conclusion

This study provides a mechanistic evaluation of SCBA and SDA in lime-based mortars. The major findings are the following:

- SCBA as a sustained pozzolan: High amorphous silica and > 86% combined oxides enabled prolonged pozzolanic reactions and superior 28-day strength and density.
- SDA as a kinetically active material: Higher specific surface area promoted rapid early-age conductivity loss, but lower reactive oxide content limited long-term strength.
- Mechanistic insight: Early electrical conductivity reduction does not directly translate into higher long-term strength; total reactive amorphous content governs sustained performance.
- Hardened properties: Both systems achieved ≥ 2 MPa compressive strength and met CS I–CS III classifications under BS EN 998-1:2016.
- Practical relevance: Lime–pozzolana mortars offer lower density and improved vapor permeability compared to OPC, supporting breathable masonry construction.
- Sustainability contribution: Valorization of agro-industrial waste supports low-carbon, locally sourced binder development.
- The study integrates early-age conductivity, mineralogy, chemistry, and mechanical performance to establish structure–reactivity–property relationships for agricultural ashes—an advancement beyond conventional strength-based evaluation.
- The study was limited to laboratory-scale testing and focused primarily on mechanical and physical properties at 28 days. Detailed quantification of amorphous phases and long-term durability behavior was beyond the present scope.
- Further research should include advanced microstructural characterization (TGA, FTIR, SEM/EDX, and Raman spectroscopy); long-term durability assessment under aggressive environmental exposures; optimized mix design; life cycle and service-life

performance assessment, and extended curing studies beyond 28 days (e.g., 56, 90, and 180 days).

Abbreviations

BET	Brunauer–Emmett–Teller
C–S–H	Calcium silicate hydrate
OPC	Ordinary Portland Cement
SCBA	Sugarcane Bagasse Ash
MPa	Mega Pascal
PSD	Particle size distribution
SCB	Sugarcane bagasse
SD	Sawdust
SDA	Sawdust Ash
SCMs	Supplementary cementitious materials
SSA	Specific surface area
XRD	X-ray diffraction
XRF	X-ray fluorescence
LOI	Loss on ignition

Acknowledgements
The authors sincerely thank the Ministry of Mining and the Ministry of Roads in Kenya for providing access to the laboratory facilities used in this study.

Author contributions
Odiwuor Vincent Onyango: designed the experiments, Performed the experiments; Analyzed andinterpreted the data; Wrote the paper.E. W, M. O, P.K : Conceived anddesigned the experiments, Contributed reagents, materials, analysis toolsor data.

Funding
This research received no external funding.

Data availability
The original contributions presented in this study are included in the article. Further inquiries can be directed to the corresponding author.

Declarations

Ethics approval and consent to participate
Not applicable. This study did not involve human and animal subjects.

Consent for publication
Not applicable.

Competing interests
The authors declare no competing interests.

Received: 6 January 2026 / Accepted: 9 July 2026
Published online: 12 July 2026

References

1. Habert G, et al. Environmental impacts and decarbonization strategies in the cement and concrete industries. Nat Reviews Earth Environ. 2020;1(11):559–73.
2. Friedlingstein P. Global carbon budget 2023. Earth Syst Sci Data. 2023. 15(12): 5301–5369.
3. Scrivener KL, John VM, Gartner EM. Eco-efficient cements: Potential economically viable solutions for a low-CO_2 cement-based materials industry. Cem Concr Res. 2018;114:2–26.
4. Elawa O, Abdellatif N, Galal T, Farahat E. Assessment of Ambient Air Quality Level at 21 Sites in the Cement Sector, Egypt. Egypt J Chem. 2022;0:0.
5. Shehata N, Mohamed OA, Sayed ET, Abdelkareem MA, Olabi AG. Geopolymer concrete as green building materials: Recent applications, sustainable development, and circular economy potentials. Sci Total Environ. 2022;836:155577.
6. Mirzaei L, Ghebrab T, Fedler CB. Review and Evaluation of Agricultural Biomass Ashes as Supplementary Cementitious Materials for Sustainable Concrete. Processes. 2025;13(11):3571.
7. Amadi IG, Mahachi J. Towards Sustainable Concrete: Current Trends and Future Projections of Supplementary Cementitious Materials in South Africa. Constr Mater. 2025;5(3):70.
8. Olaiya BC, Lawan MM, Olonade KA, Segun OO. An overview of the use and process for enhancing the pozzolanic performance of industrial and agricultural wastes in concrete. Discover Appl Sci. 2025. 7: 164.
9. Malhotra S, Kanoungo A, Goyal A. Utilization of Industrial and Agricultural Wastes to Enhance the Properties of Concrete—A Review, Lecture Notes in Civil Engineering. 2023. 91–101.
10. Prabhath N, Damruwan H-GH, Lewangamage KR, Sewwandi N. Investigation of pozzolanic properties of sugarcane Bagasse ash for commercial applications. ACS Omega, 2023. 8(13):12052-61.

11. Assumptor O, Masika E, Thiong'K. Probing Optimal Blends of Pozzolans to Develop Supplementary Cementing Material Within Busia County, Kenya. J Appl Phys (IOSR-JAP) e. 2020;12(2):59–69.
12. Hossain MM, Karim MR, Elahi MMA, Mohd MF, Zain. Water absorption and sorptivity of alkali-activated ternary blended composite binder. J Building Eng. 2020;31:101370.
13. Costa L et al. Effect of partial replacement with thermally processed sugar cane bagasse on the properties of mortars. Matéria. 2017. 22: e11785.
14. Ghosh B. Sugarcane Bagasse Ash as a Partial Replacement for Cement in Concrete. AMC Indian J Civil Eng. 2024;7(1):30.
15. Bhardwaj N, Kasilingam S. Performance of agro-waste sugarcane bagasse ash in concrete under durability tests. Acta Scientiarum Polonorum Architectura. 2025;24:92–101.
16. Majeed SS. Formulating Eco-Friendly Foamed Mortar by Incorporating Sawdust Ash as a Partial Cement Replacement. Sustainability. 2024;16(7):2612–2612.
17. Soomro R, Qureshi S, Arisar U, Investigation on the mechanical properties of concrete with partial replacement of fine aggregate by sawdust ash for sustainable construction. Pak J Sci Res. 2024;4(2):162–70.
18. Elinwa AU. Sawdust ash-Conplast admixed concrete: Compressive strength and acid-sulfate evaluation. Mater Chem Phys. 2025;346:131394.
19. KS EAS 18 – 1. Kenya Standard Test Method for Oxides Specification of Hydraulic Cement. Kenya Bureau of Standards. Nairobi, Kenya; 2017.
20. KS 02 1263. Specification for Portland Pozzolana Cements. Kenya Bureau of Standards. Nairobi, Kenya; 1993.
21. John LK. Pozzolana Cement Obtained by Calcining Raw Clays/Rice Husks Mixtures. Ku ac ke, 2013.
22. Marangu JM, Muthengia JWJW, Thiong OJK. Performance of Potential Pozzolanic Cement in Chloride Media. IOSR J Appl Chem. 2014;7(2):36–44.
23. Luxán MP, Madruga F, Saavedra J. Rapid evaluation of pozzolanic activity of natural products by conductivity measurement. Cem Concr Res. 1989;19(1):63–8.
24. Musyimi NF, Karanja J, Wachira M, Mulwa M. Pozzolanicity and Compressive Strength Performance of Kibwezi Bricks Based on Cement. IOSR J Appl Chem (IOSR-JAC). 2016;9(2):28–32.
25. KS EAS 2168-1. Kenya Standard Test Method, Composition, Specification, and Conformity Criteria of Masonry Cement. Kenya Bureau of Standards. Nairobi, Kenya; 2020.
26. KS EAS 148-1, Cement-Test Methods. Part 1: Determination of Strength. Kenya Bureau of Standards. Nairobi, Kenya; 2017.
27. BS 1881 – 114. Methods for determination of density of hardened concrete. British Standards Institution; 1983.
28. BS, 1881 – 122. Method for determination of water absorption. Br Standard Institution, 2011.
29. Cordeiro GC, Toledo Filho RD, Tavares LM, de Fairbairn E, Hempel S. Influence of particle size and specific surface area on the pozzolanic activity of residual rice husk ash. Cem Concr Compos. 2011;33(5):529–34.
30. Pavía S, Figueiredo RL. A study of the parameters that determine the reactivity of sugarcane bagasse ashes (SCBA) for use as a binder in construction. SN Appl Sci. 2020. 2: 1515.
31. Walker R, Pavía S. Physical properties and reactivity of pozzolans, and their influence on the properties of lime–pozzolan pastes. Mater Struct. 2010;44(6):1139–50.
32. Yaseen N. Exploring the potential of sugarcane bagasse ash as a sustainable supplementary cementitious material: Experimental investigation and statistical analysis. Results Chem. 2024;10:101723.
33. Nayak JR, Gołaszewska M, Bochen J. Physical and Mechanical Performance of Mortar with Rice Husk Ash and Sugarcane Bagasse Ash as Partial Cement Replacement. Materials. 2025;18(20):4758.
34. Jittin V, Bahurudeen A. Evaluation of rheological and durability characteristics of sugarcane bagasse ash and rice husk ash-based binary and ternary cementitious system. Constr Build Mater. 2022;317:125965.
35. ASTM C618. Standard Specification for Coal Fly Ash and Raw or Calcined Natural Pozzolan for Use in Concrete, 2023.
36. Raheem AA, Ige AI. Chemical composition and physicomechanical characteristics of sawdust ash blended cement. J Building Eng. 2019;21:404–8.
37. Ogork EN, Ayuba S. Influence of sawdust ash (SDA) as admixture in cement paste and concrete. IJISET—International J Innovative Sci Eng Technol. 2014. 1: 736-43.
38. Olaiya BC, Lawan MM, Olonade KA. Utilization of sawdust composites in construction—a review. SN Appl Sci. 2023. 5: 140.
39. Asif I, Hussain MU, Khan AA, Ashar M, Shahid Z. Utilization of Sawdust Ash as an Additive of Cement in Concrete and Study of Its Mechanical Properties. Memoria Investigaciones en Ingenieria. no. 2024;26:54–69.
40. Niyomukiza JB, Yasir Y. Effects of using sawdust ash as a stabilizer for expansive soils. E3S Web of Conferences. 2023. 448: 03075
41. Ryssen V, Ndlovu H. Wood ash in livestock nutrition: 1. Factors affecting the mineral composition of wood ash. Appl Anim Husb Rural Dev. 2018;11(1):53–61.
42. Jurić KK, Carević I, Serdar M, Štirmer N. Feasibility of using pozzolanicity tests to assess reactivity of wood biomass fly ashes. J Croatian Association Civil Eng. 2021;72(12):1145–53.
43. Neville AM, Brooks JJ. Concrete technology. Harlow, England; New York: Prentice Hall; 2010.
44. Garcia LI, Palomo A, Fernandez JA. Alkali–aggregate reaction in activated Fly Ash systems. Cem Concr Res. 2007. 37(2):175-83.
45. Chusilp N, Jaturapitakkul C, Kiattikomol K. Effects of LOI of ground bagasse ash on the compressive strength and sulfate resistance of mortars. Constr Build Mater. 2009;23(12):3523–31.
46. Cordeiro GC, Toledo Filho RD, Tavares LM, Fairbairn EMR. Pozzolanic activity and filler effect of sugar cane bagasse ash in Portland cement and lime mortars. Cem Concr Compos. 2008;30(5):410–8.
47. Francioso V, Lemos-Micolta ED, Elgaali HH, Moro C, Rojas-Manzano MA, Velay-Lizancos M. Valorization of Sugarcane Bagasse Ash as an Alternative SCM: Effect of Particle Size, Temperature-Crossover Effect Mitigation & Cost Analysis. Sustainability. 2024;16(21):9370.
48. Meko B, Ighalo JO. Utilization of Cordia Africana wood sawdust ash as partial cement replacement in C 25 concrete. Clean Mater. 2021;1:100012.
49. Taylor HFW. Cement Chemistry. 2nd Edition, Thomas Telford Publishing, London, 361. References - Scientific Research Publishing, 1997.
50. Elinwa AU, Mamuda AM. Sawdust Ash as Powder Material for Self-Compacting Concrete Containing Naphthalene Sulfonate. Adv Civil Eng. 2014;2014:1–8.

51. Rajamma R, Ball RJ, Tarelho LAC, Allen GC, Labrincha JA, Ferreira VM. Characterisation and use of biomass fly ash in cement-based materials. J Hazard Mater. 2009;172:2–3.
52. Berra M, Mangialardi T, Paolini AE. Reuse of woody biomass fly ash in cement-based materials. Constr Build Mater. 2015;76:286–96.
53. Demis S, Tapali JG, Papadakis VG. An investigation of the effectiveness of the utilization of biomass ashes as pozzolanic materials. Constr Build Mater. 2014;68:291–300.
54. Neville AM, Brooks JJ. Concrete technology. Harlow, England; New York: Prentice Hall; 2010.
55. Meko B, Ighalo JO. Utilization of Cordia Africana wood sawdust ash as partial cement replacement in C25 concrete. Clean Mater. 2021;1:100012.
56. Zúniga A, Eires R, Malheiro R. New Lime-Based Hybrid Composite of Sugarcane Bagasse and Hemp as Aggregates. Resources. 2023;12(5):55.
57. Sales A, Lima SA. Use of Brazilian sugarcane bagasse ash in concrete as sand replacement. Waste Manag. 2010;30(6):1114–22.
58. BS EN 998-1. Specification for mortar for masonry: Rendering and plastering mortar. Br Stand Institution, 2016.
59. Massazza F. Pozzolana and Pozzolanic Cements. In Hewlett, P.C., Ed., Lea's Chemistry of Cement and Concrete, 4th Edition, Elsevier, London, 471–635. References—Scientific Research Publishing, 2019.
60. Ghosh B. Sugarcane Bagasse Ash as a Partial Replacement for Cement in Concrete. AMC Indian J Civil Eng. 2024;7(1):30.
61. Munyao OM. Microbial effects on physico-mechanical and microstructural properties of commercial portland cements. Ku ac ke, 2022.

Publisher's Note